DOI 10.1007/s11041-018-0274-6
Metal Science and Heat Treatment, Vol. 60, Nos. 5 – 6, September, 2018 (Russian Original Nos. 5 – 6, May – June, 2018)

UDC 669.295:621.785.53

EFFECT OF VACUUM ION-PLASMA TREATMENT ON SURFACE LAYER STRUCTURE, CORROSION AND EROSION RESISTANCE OF TITANIUM ALLOY WITH INTERMETALLIC α_2-PHASE

A. M. Mamonov,[1] S. M. Sarychev,[2] S. S. Slezov,[1] and Yu. V. Chernyshova[1]

Translated from *Metallovedenie i Termicheskaya Obrabotka Metallov*, No. 5, pp. 17 – 24, May, 2018.

Results are provided for a study of the effect of vacuum ion-plasma nitriding on the phase composition, structure, microhardness, salt corrosion resistance, and erosion resistance of alloy Ti – 14Al – 3Nb – 3V – 0.5Zr with an original bimodal structure and different surface microgeometry. It is shown that with an increase in nitriding temperature from 550 to 650°C the content of Ti_2N nitrides in the surface layer increases and Ti_3AlN nitride in formed, which raises the microhardness but reduces the thickness of the hardened diffusion zone; pores appear in the surface at 650°C. Vacuum ion-plasma nitriding is shown to raise substantially the resistance of specimens of alloy Ti – 14Al – 3Nb – 3V – 0.5Zr with a polished surface to salt corrosion. Additional nitriding after deposition of a TiN coating improves ground specimens salt corrosion resistance. Vacuum ion-plasma nitriding with additional deposition of a TiN coating increases the resistance of specimens with polished and ground surfaces to erosive action.

Key words: titanium aluminide, vacuum ion-plasma nitriding, corrosion, microhardness, structure, phase composition.

INTRODUCTION

Titanium alloys with a high volume fraction of intermetallic α_2-phase base on titanium aluminide Ti_3Al are traditionally considered as promising materials for use in aero gas turbine engines and power generation installations [1 – 3]. Surpassing commercial titanium alloys with respect to specific heat resistance, high-temperature strength, and level of operating temperature these materials have lower production ductility, which considerably complicates the preparation of the required wrought semiproducts and objects. Another serious problem, retarding use of these alloys, especially with an $\alpha + \alpha_2$-structure (i.e., containing from 7 to 14 wt.% aluminum) is the low thermal stability at working temperatures [4]. Work of Russian and overseas researchers has been performed for solution of these and other problems for alloys of these classes [5 – 7].

However, it is desirable to consider the possibility of using alloys containing aluminum, exceeding its limiting solubility in α-titanium in fields not connected with action of high temperature. One of these fields is production of objects for medicinal purposes, in particular highly loaded implants and surgical instruments for orthopedics and traumatology. In order to prepare implants there is traditional use of titanium alloys with normal or reduced elasticity modulus [8 – 10].

Concerning medical instruments for endo-prostheses, then the main specifications to be considered are their corrosion resistance, hardness, specific strength, wear resistance, and also structural stiffness, which is determined by tool geometry and material elasticity modulus. It is well known that aluminum increases the elasticity modulus of titanium alloys due to increasing interatomic bond strength in a titanium HP-lattice. On alloying with aluminum up to 10 wt.% the normal elasticity modulus for α-titanium increases by 20% [11]. As a result of this use of high modulus titanium alloys with increased aluminum content is very promising for preparing large orthopedic cutting tools. This makes it possible to create reliable light ergonomically high resource surgical instrumentation.

The collection of requirements for object properties gives a rise to a requirement for forming within them a composite structural state with which the optimum structure of a material volume, providing good strength and fatigue properties, and crack resistance, is combined with a graded modified surface layer and functional coatings giving high hard-

[1] Moscow Aviation Institute (National Research University), Moscow, Russia (e-mail: mitom@implants.ru).
[2] Implant MT, JSC, Moscow, Russia.

ness and wear resistance. It is apparent that in order to create these structural states it is necessary to use complex technology.

One of the most promising comprehensive technologies for this group of titanium alloys is that consisting of a sequence of using thermal hydrogen treatment (THT) and vacuum ion plasma nitriding (VIPN) with controlled, energy, concentration, and kinetic parameters [12]. Use of hydrogen technology for preparing and treating wrought semiproducts, based on the hydrogen plastification [13 – 18], makes it possible to resolve the problem of production ductility for these alloys.

The possibility has been considered in [16] of creating by means of THT bimodal structures in alloy based on titanium aluminide Ti_3Al. Apart from a good combination of strength and ductility properties, this structure should provide greater efficiency for vacuum ion-plasma nitriding due to presence of a finely dispersed structure of components of secondary $\alpha(\alpha_2)$-phase with a lower degree of ordering than in primary ordered α_2-phase. In the case the volume fraction of secondary α_2-phase within the alloy structure after THT comprised 40 – 50%.

It is well known that use of vacuum ion-plasma nitriding is most effective for improving the tribological properties of titanium alloys, including wear resistance. However, until now this technology has only been developed for structural titanium alloys and applied to friction assemblies of medicinal implants and the elements of joints of limited mobility in aviation engineering.

Currently [17 – 19] solid phase technology is being created for creating graded surface structures in titanium alloys by alloying with nitrogen during low-temperature ion nitriding in a gas atmosphere (mixture of nitrogen and argon) with application of an electric field with low voltage potential difference. Use of this technology makes it possible to provide controlled alloying with nitrogen of the surface of finished objects at 550 – 600°C and short exposures (up to 1 h), which does not affect either the surface microgeometry or the structure formed within the volume of a component in the preceding production stages for preparing and treating semiproducts.

The of the present work[3] is a study of the effect of vacuum ion-plasma nitriding on phase composition, structure, microhardness, salt corrosion resistance, and erosion resistance of alloy Ti – 14% Al – 3% Nb – 3% V – 0.5% Zr with an initial bimodal structure and different surface microgeometry.

METHODS OF STUDY

Research was performed on specimens of alloy Ti – 14Al – 3Nb – 3V – 0.5Zr (wt.%) [20], cut from hot-rolled bar 50 mm in diameter. Specimen workpieces were subjected to hydrogen thermal treatment by the Sieverts method [13] by a regime providing preparation of a bimodal structure with a volume faction of primary globular α_2-phase with a size of 3 – 5 μm of about 50% and a finely dispersed mixture of $\alpha(\alpha_2)$- and β-phases [16]. Specimens 2 – 3 mm thick were cut from workpieces. In order to determine the effect of original surface micro-geometry on the properties studied, specimens were mechanically ground with preparation of roughness parameter R_a = 0.15 – 0.21 μm, and subsequent polishing with diamond paste to R_a = 0.04 μm. Parameter R_a was measured in a Hommel Tester T500 instrument on a linear base of 0.8 mm.

Vacuum ion-plasma nitriding was performed in Bulat-6T unit with controlled mixture of nitrogen and argon at temperatures from 550 to 650°C with preliminary ion cleaning.

Corrosion resistance was studied by a potentiodynamic method [21, 22] in 3% aqueous NaCl solution at room temperature using a PI-50-1.1 potentiostat, a three-electrode cell, a subsidiary electrode of platinum wire, and a silver chloride electrode as the reference electrode. The steady-state value of electrode potential (E_{st}), pitting formation potential (E_{po}) and passive state current density (i_{pas}) were determined.

A specimen surface after nitriding and corrosion tests was studied in a Axio-Observer. A1m light microscope with software for analyzing images NEXSIS ImageExpert Pro 3.

A specimen surface phase composition after nitriding was determined by x-ray diffractometry in DRON-4 and DRON-7 diffractometers with filtered copper K_α-radiation.

Specimen microhardness $HV_{0.05}$ was measured in a Micromet 5101 instrument. In order to determine the thickness of the strengthened (modified with nitrogen) surface layer an oblique angle microsection was used with an angle of 3°.

Specimen resistance to erosive action (by analogy with wear resistance) was evaluated by blowing the surface with a stream of compressed air, containing microparticles with a size of about 100 μm of aluminum silicate glass (dull finishing) with subsequent measurement of parameter R_a.

RESULTS AND DISCUSSION

In selecting vacuum ion-plasma nitriding (VIPN) regimes results of work in [12, 17 – 19] were considered, and also known general features of titanium alloy nitriding with a different degree of alloying with aluminum and β-stabilizers [23].

The main difference of the test alloy from structural alloys based on titanium is an ordered condition of α_2-phase, although the primary α_2-phase bimodal structure contains a greater amount of aluminum than secondary finely dispersed $\alpha(\alpha_2)$-phase [24]. The interatomic bond strength in the ordered α_2-phase lattice is markedly greater than in α-phase, due to development of a covalent component. This leads to

[3] Work was conducted with use of equipment of the resource center for collective usage "Aerospace materials and technology" of the Moscow Aviation Institute.

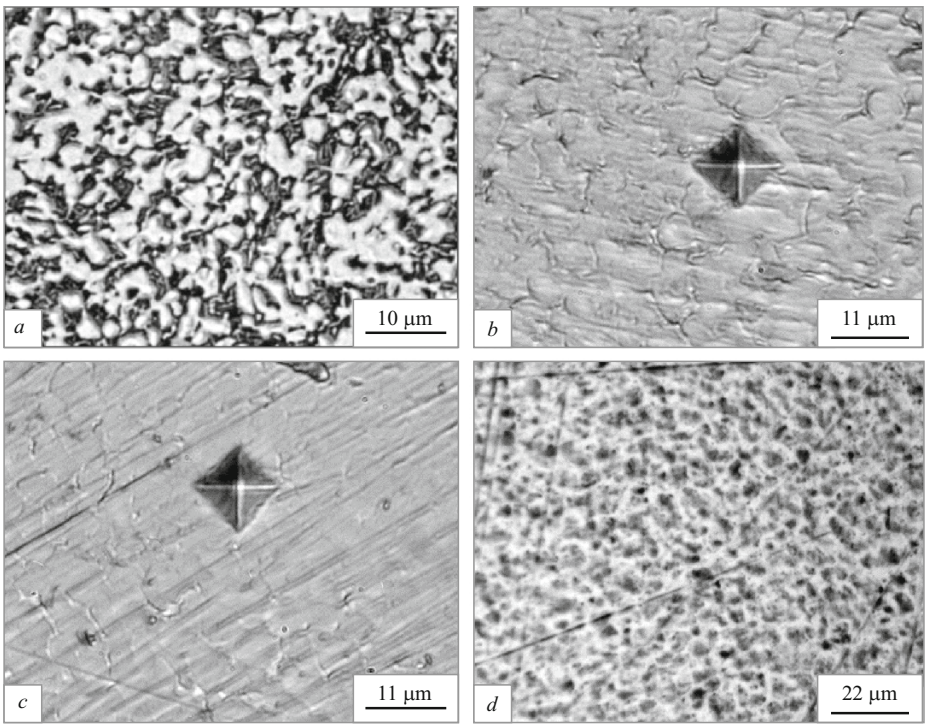

Fig. 1. Microstructure of the volume (*a*) and surface (*b* – *d*) of specimens subjected to VIPN by different regimes: *b*) 550°C, 1 h; *c*) 600°C, 1 h; *d*) 650°C, 40 min.

partial blocking of the intermodal lattice, increasing nitrogen diffusion activation energy and reducing its intensity, and also reducing nitrogen solubility, especially in primary α_2-phase. Under these conditions the predominant role of forming a diffusion zone should be played by a finely-dispersed mixture of β- and secondary $\alpha(\alpha_2)$-phases, having a high extent of interphase boundaries, and being a good diffusion "channel." In addition, it is well known that the diffusion coefficient in β-phase, even containing alloying elements, is markedly higher than in α-phase [25]. However, it should be considered that in this case nitrogen diffusion should initiate $\beta \rightarrow \alpha$-transformation, which will be accompanied by coarsening of $\alpha(\alpha_2)$-phase particles and possible coalescence that as a result leads to a reduction in the proportion of finely dispersed mixture of $\alpha(\alpha_2)$- and β-phases in a bimodal structure and formation within the surface layer of a structure close to equiaxed.

Considering the reasoning provided above, and also the fact that the best results for wear and corrosion resistance of nitrided structural alloys [19, 23] have been obtained with a VIPN temperature of 550 – 580°C, the following treatment regimes were selected: *1*) 550°C, 40 min; *2*) 550°C, 60 min; *3*) 600°C, 60 min; *4*) 650°C, 40 min.

The structure within the volume of an alloy specimen before VIPN and the structure of the surface after nitriding by different regimes is given in Fig. 1. With nitriding temperatures of 550 and 600°C ground and polished specimens have a dense uniform surface of light yellow color without significant defects, i.e., pores and other discontinuities (Fig. 1*b* and *c*). Nitriding at 650°C leads to formation at a specimen surface of a considerable number of pores (Fig. 1*d*), and the surface becomes matte and has a more intense yellow color. This develops to the greatest extent in specimens after mechanical grinding. Roughness parameters for an original polished surface increase less markedly the higher the nitriding temperature: up to 0.06 – 0.07 μm at 550 and 600°C, and up to 0.10 μm at 650°C (Table 1).

Results of x-ray studies of the phase composition of the surface layer of a specimen are provided in Fig. 2. The phase composition of specimens treated by regimes *1* and *2* is represented by α_2-, β-, and $\varepsilon(Ti_2N)$-phases (Fig. 2*a*). No marked difference in amount of nitride was revealed. Comparison of the integral intensity and angular position of α_2- and β-phase reflections makes it possible to suggest that with an increase in nitriding duration and 550°C from 40 to

TABLE 1. Surface properties of Ti – 14Al – 3Nb – 3V – 0.5Zr Alloy Specimens after Vacuum Ion-Plasma Nitriding

VIPN by different regimes	$HV_{0.05}$, MPa	R_a, μm	h, μm
Original condition	3800	0.04/0.18	–
550°C, 40 min	4780	0.05/0.19	90/85
550°C, 1 h	4830	0.06/0.19	95/90
600°C, 1 h	5500	0.07/0.20	60/50
650°C, 40 min	5850	0.10/0.34	50/40

Notations: $HV_{0.05}$ is polished specimen average microhardness, R_a is average roughness parameter, h is strengthened layer thickness.

Note. R_a and h provided in the numerator for original ground, and in the denominator for original polished surfaces.

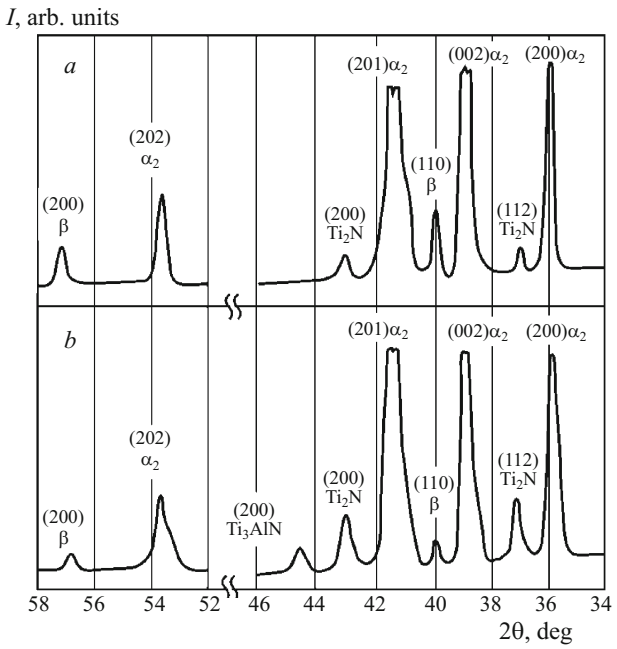

Fig. 2. Areas of diffraction patterns for specimens after VIPN at 550°C, 30 min (*a*) and 650°C, 40 min (*b*) (*I* is emission intensity).

60 min there is some reduction in the amount of β-phase and an increase in the nitrogen content in α_2-phase. The light yellow color of a specimen surface indirectly points to presence within it of titanium nitride TiN, although its layer is exceptionally thin, which does not make it possible to reveal it by an x-ray method.

Within the structure of specimens nitrided at 600 and 650°C (regimes *3* and *4*), apart from nitride Ti_2N, a complex nitride Ti_3AlN was detected (Fig. 2*b*). The amount of Ti_2N nitride increases with an increase in nitriding temperature. In addition, asymmetry is revealed for α_2-phase reflections, expressed within them as broadening from the direction of smaller Bragg angles. This points to dissolution of nitrogen predominantly in finely dispersed $\alpha(\alpha_2)$-phase. The amount of β-phase decreases with an increase in nitriding temperature.

The average microhardness of specimens in relation to surface preparation and VIPN regime is given in Table 1. The average microhardness with an increase in temperature and nitriding duration increases and reaches a maximum at 650°C, which is connected with an increase in the amount of nitride within a surface layer (Table 1).

The greatest thickness of the zone strengthened with nitrogen (diffusion) is reached for ground specimens nitrided at 550°C (Table 1 and Fig. 3*a* and *b*). An increase in temperature to 600 and 650°C leads to a sharp (by a factor of 1.5 – 2) reduction in the extent of the diffusion zone (Fig. 3*c* and *d*), which is probably caused by formation of a considerable amount of stable TiN and Ti_3AlN nitrides stable at these temperatures in various stages of the nitriding process.

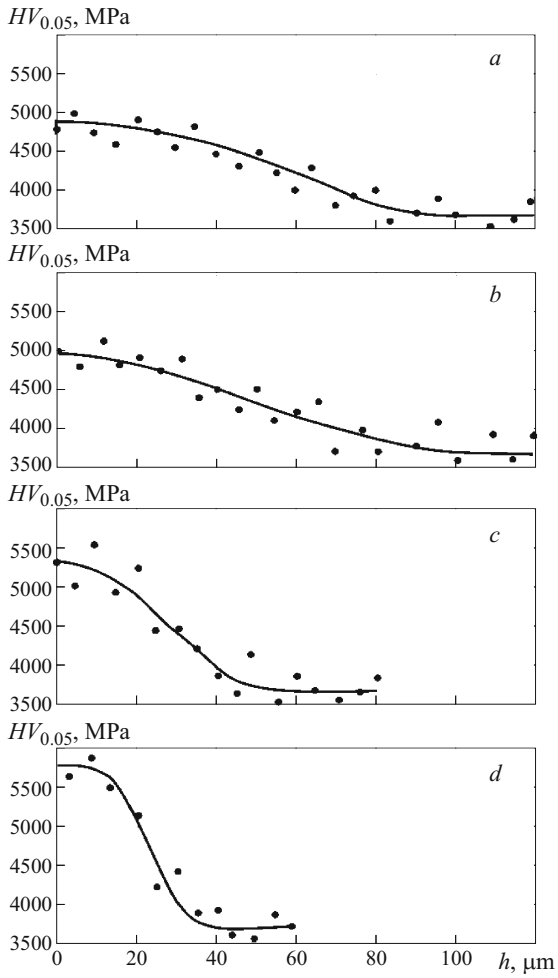

Fig. 3. Microhardness distribution through the thickness of a nitrided layer on originally polished specimens subjected to VIPN by regimes *1* (*a*), *2* (*b*), *3* (*c*), and *4* (*d*) (*h* is distance from surface).

Taking account of the results obtained for microhardness and modified strengthened layer thickness for corrosion studies, specimens with an original ground and polished surface, and also specimens after VIPN at 600°C were selected. In one part of nitrided specimens a layer of titanium nitride TiN was applied additionally by a condensation method.

Before the start of testing all specimens were held in NaCl solution for 2 h in order to achieve a steady value of electrode potential.

Results of potentiodynamic for specimens are provided in Table 2. Negative values of steady state potential E_{st} only apply to polished specimens.

Formation at a polished specimen surface during VIPN of a nitrided layer with nitrides ε-Ti_2N, δ-TiN, and Ti_3AlN leads to a significant (594 mV) shift in E_{st} into the positive region (Table 2). With additional application at a polished specimen surface after VIPN of a coating of titanium mononitride TiN, lower values of steady state potential are observed compared with nitrided specimens (Table 2).

TABLE 2. Results of Potentiodynamic Tests for Ti – 14Al – 3Nb – 3V – 0.5Zr Alloy Specimens in Aqueous NaCl Solution

Treatment	Specimen electrochemical characteristics			Specimen external appearance after testing
	E_{st}, mV	E_{po}, mV	i_{pas}, μA/cm^2	
Ground	+ 324	+ 1408	$1.46 \times 10^{-6} – 1.49 \times 10^{-6}$	Pitting present, blue spots
Mechanical polishing	– 126	Sample not obtained	$8.56 \times 10^{-7} – 7.85 \times 10^{-6}$	No color change or damage
Grinding + VIPN	+ 318	+ 1458	$9.09 \times 10^{-8} – 4.55 \times 10^{-6}$	Color change from light-yellow to dark-yellow, pitting present, blue spots
Polishing + VIPN	+ 468	Sample not obtained	$3.75 \times 10^{-8} – 1.31 \times 10^{-5}$	Color change from light-yellow to dark-yellow, no damage
Grinding + VIPN + TiN	+ 363	+ 2000	$1.52 \times 10^{-8} – 1.5 \times 10^{-5}$	Color change from yellow to dark-yellow with grey spots, pitting present
Polishing + VIPN + TiN	+ 388	Sample not obtained	$2.75 \times 10^{-8} – 3.85 \times 10^{-5}$	Color change from yellow to brown, no damage

The steady state potential of ground specimens, subjected to VIPN, is close to the steady state potential for original specimens. After additional coating application of titanium mononitride TiN an increase is observed in the steady state potential for specimens compared with the nitrided condition (Table 2).

Results of studies have shown that the corrosion process proceeds with anodic control, i.e., the anodic reaction is limiting (limiting corrosion rate). In view of this in subsequent studies anodic polarization curves were used (Fig. 4) in order to evaluate the effect of treatment method on specimen corrosion resistance.

As these studies have shown, anodic polarization curves, obtained for specimens of alloy Ti – 14Al – 3Nb – 3V – 0.5Zr, do not have fundamental differences from the polarization curves for structural titanium alloys. Anodic polarization curves for ground specimens have a clearly defined region of a passive condition, the current density of which is close to that obtained for titanium alloys VT6 and VT20 [12].

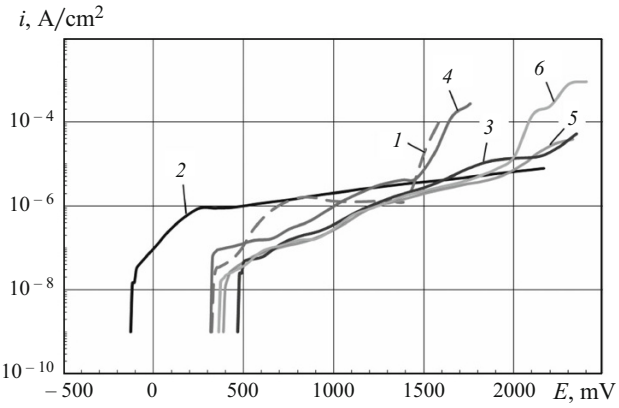

Fig. 4. Anodic polarization curves for Ti – 14Al – 3Nb – 3V – 0.5Zr alloy specimens obtained in 3% NaCl aqueous solution (*i* is current density, *E* is corrosion potential): *1*) grinding; *2*) polishing; *3*) polishing + VIPN; *4*) grinding + VIPN; *5*) polishing + VIPN + TiN; *6*) grinding + VIPN + TiN.

On reaching a potential of value +1408 mV on the anodic curve a sharp increase in current density is observed, which points to presence of pitting formation. A study of a specimen surface by means of a light microscope confirmed presence within it of local corrosion damage, i.e., pitting, and development of blue spots was observed in areas of its formation (Fig. 5*a*, Table 2).

For specimens subjected to mechanical polishing of the surface, the anodic polarization curve has an extended region of passive condition, and pitting formation at a specimen surface is not observed.

Vacuum ion plasma nitriding leads to a significant (for polished specimens by almost an order to magnitude) reduction in current density in the passive region (see Fig. 4). On anodic curves for polished specimens after use of VIPN an extended passive region is retained, and there is no pitting formation at the surface (Fig. 5*b*).

VIPN of ground specimens hardly changes the pitting formation potential (see Table 2 and Fig. 5*c*). After corrosion tests at a surface there is formation of pitting and blue spots appear.

Application at the surface of polished specimens after VIPN of a layer of TiN does not cause significant changes to their corrosion resistance. The current density of the passive condition is almost unchanged, and there is almost no pitting at the surface (Fig. 5*d*).

With application of a TiN coating to ground specimens the current density of the passive region decreases, but the process of pitting formation is not entirely suppressed. Pitting formation is observed at potentials of the order of 2000 mV. Therefore, use of VIPN makes it possible to improve significantly the corrosion properties of specimens of alloy Ti – 14Al – 3Nb – 3V – 0.5Zr, i.e., to increase their steady state potential and to reduce by almost an order of magnitude the current density of the passive condition. In this case polished specimens after use of VIPN have better corrosion resistance.

Application of a coating of titanium mononitride TiN after VIPN does have a significant effect on the corrosion re-

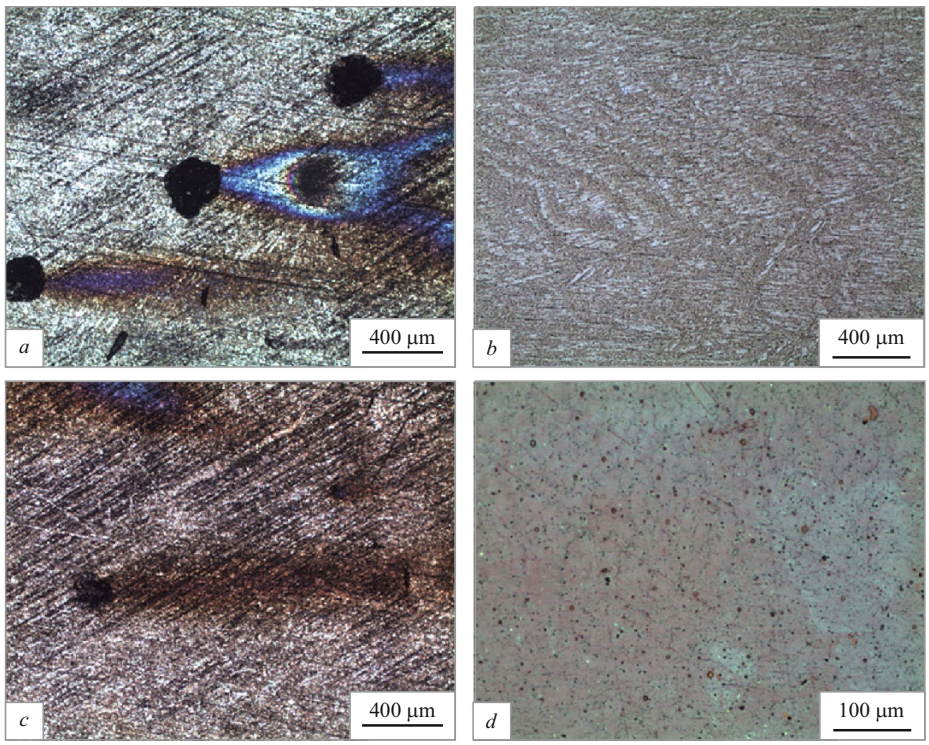

Fig. 5. External appearance of Ti – 14Al – 3Nb – 3V – 0.5Zr alloy specimen surface after potentiodynamic tests in 3% NaCl aqueous solution: *a*) grinding; *b*) polishing + VIPN; *c*) grinding + VIPN; *d*) polishing + VIPN + TiN.

sistance of polished specimens, and the resistance of ground specimens in this case is improved, i.e., there is a reduction in current density of the passive state i_{pas} and an increase in pitting formation potential E_{po} .

Specimens with ground and polished surfaces, specimens after VIPN at 600°C for 60 min, and specimens with additional application of a TiN-coating, were subjected to erosive action. The resistance to erosive action was evaluated from the change in surface roughness parameter. Test results are provided in Table 3.

The degree of the effect of erosive action on specimen surface condition is clearly illustrated in Fig. 6.

Specimens with an original polished surface exhibit the least resistance to erosive action. VIPN, especially combined with additional application of titanium nitride, improves erosion resistance to the greatest extent (Fig. 6). Surface grinding considerably improves erosion resistance, apparently due to strengthening a surface as a result of work hardening. VIPN of these specimens hardly improves erosion resistance since the thermal action of nitriding (600°C) overcomes work hardening. Application of titanium nitride to ground specimens provides a significant increase in microhardness and a minimum change in surface roughness, although in this case the relative increase in erosion resistance is not as significant as in the case of specimens with a polished surface (Fig. 6).

TABLE 3. Effect of Erosive Action on Roughness Parameter R_a for Ti – 14Al – 3Nb – 3V – 0.5Zr Alloy Specimens after Different Treatment

Treatment	Original R_a , μm	R_a after action, μm
Grinding	0.20	0.54
Polishing	0.04	0.92
Grinding + VIPN	0.20	0.58
Polishing + VIPN	0.07	0.59
Grinding + VIPN + TiN	0.26	0.48
Polishing + VIPN + TiN	0.08	0.41

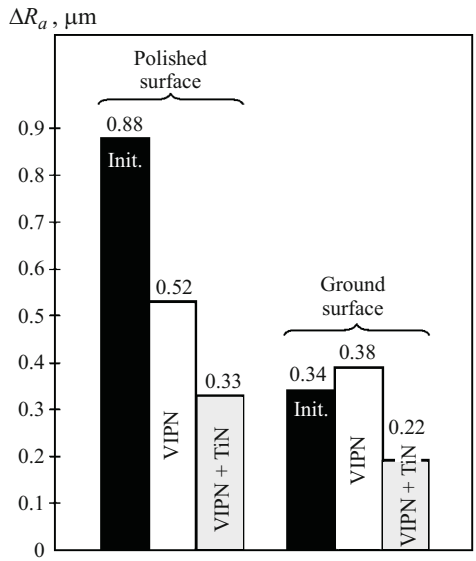

Fig. 6. Roughness parameter for Ti – 14Al – 3Nb – 3V – 0.5Zr alloy specimens subjected to different treatment after erosion resistance testing.

CONCLUSIONS

1. An increase in vacuum ion plasma nitriding temperature for alloy Ti – 14Al – 3Nb – 3V – 0.5Zr from 550 to 650°C leads to an increase of the amount of Ti_2N nitride in its surface layer and formation of Ti_3AlN nitride, which facilitates an increase in microhardness, although the reduction in depth of strengthened diffusion zone at 620°C causes pore formation in the surface.

2. Vacuum ion plasma nitriding facilitates to the greatest extent an increase in resistance to salt corrosion of specimens of alloy Ti – 14Al – 3Nb – 3V – 0.5Zr with a polished surface. Addition after nitriding of application of a titanium nitride TiN coating leads to an increase in slat corrosion resistance for ground specimens.

3. Vacuum ion plasma nitriding with additional application of a TiN coating improves to the greats extent the resistance of alloy Ti – 14Al – 3Nb – 3V – 0.5Zr with both polished and with ground surfaces towards erosive action.

REFERENCES

1. E. N. Kablov, "Strategic directions for developing materials and technology of their processing in the period up to 2030," *Aviats. Mater. Tekhnol.*, No. S, 7 – 17 (2012).
2. N. A. Nochovnaya and V. I. Ivanov, "Intermetallics based on titanium. Analysis of the state of the question," *Titan*, No. 1, 7 – 14 (2007).
3. A. A. Il'in, V. A. Kolachev, and I. S. Pol'kin, *Titanium Alloys. Composition, Structure, and Properties: Handbook* [in Russian], VILS – MATI, Moscow (2009).
4. A. A. Ilyin, A. M. Mamonov, Y. N. Kusakina, and V. K. Nosov, "Hydrogen influence on the structure of high-temperature strength titanium alloy with intermetallic hardening," in: *EUROMAT-97. Maastricht-NL. April 1997. Proc. 5th European Conference on Advanced Materials, Processes and Applications* (1997), pp. 307 – 310.
5. Wang Bin, Tiancong Jia, and Dunxue Zou, "A study on long-term stability of Ti_3Al – Nb – V – Mo alloy," *Mater. Sci. Eng. A*, **153**(1), 422 – 426 (1992).
6. L. S. Apgar, C. I. Yolton, and M. Sagib, "Microstructure and property modification of cast alpha-2 titanium alloys by thermochemical processing with hydrogen," in: *Titanium–92 Science and Technology: Processing 7th World Titanium Conference (San-Diego, California June 29 – July 2, 1992)*, Minerals, Metals and Materials Society, Warrendale, Pa. (1993), Vol. 2, pp. 1331 – 1335.
7. G. Lutjering, G. Proske, and G. Terlinde, "Influence of microstructure, texture and environment on tensile properties of super alpha-2," in: *Titanium–95 Science and Technology: Proceedings of the Eighth World Conference on Titanium (Birmingham, UK 22 – 26 October 1995)*, Institute of Materials (1996), Vol. 1, pp. 332 – 339.
8. M. Niinomi, "Titanium alloys for biomedical, dental and healthcare applications," in: *Ti–2007 Science and Technology: Proceedings of the 11th World Conference on Titanium (Kyoto, Japan, 3 – 7 June 2007)*, The Japan Institute of Metals (2007), Vol. 2, pp. 1417 – 1425.
9. M. Tahara, H. Y. Kim, T. Inamura, et al., "Effect of addition on mechanical properties of Ti – 20Nb – 4Zr – 2Ta (at%) biomedical superelastic alloy," in: *Ti–2007 Science and Technology: Proceedings of the 11th World Conference on Titanium (Kyoto, Japan, 3 – 7 June 2007)*, The Japan Institute of Metals (2007), Vol. 2, pp. 1453 – 1454.
10. Ding Dongyan, Liu Hegang, Ning Congqin, and Li Zhaohui, "Development of biomedical Ti – Cr alloys with changeable young's modulus via deformation-induced transformation," in: *Ti–2011: Proceedings of the 12th World Conference on Titanium (Beijing, China, 19 – 24 June 2011)*, The Japan Institute of Metals (2011), Vol. 3, pp. 2046 – 2050.
11. E. V. Collins, *Physical Metallurgy of Titanium Alloys* [Russian translation], Metallurgiya, Moscow (1298).
12. A. A. Il'in, A. M. Mamonov, V. N. Karpov, et al., "Comprehensive technology for creating wear resistant highly loaded components of endoprostheses of large joints of titanium alloys," *Tekhnol. Mashinotr.*, No. 9, 43 – 47 (2007).
13. A. A. Il'in, V. A. Kolachev, V. K. Nosov, and A. M. Mamonov, *Hydrogen Technology of Titanium Alloys* [in Russian], MISiS, Moscow (2002).
14. V. K. Nosov and B. A. Kolachev, *Hydrogen Plastification During Hot Deformation of Titanium Alloys* [in Russian], Metallurgiya, Moscow (1986).
15. A. A. Ilyin, V. K. Nosov, and S. V. Scvortsova, "Hydrogen technology of semiproducts and finished goods production from high-strength titanium alloys," in: *Advances in the Science and Technology of Titanium Alloy Processing*, TMS, Anaheim, California (1997), pp. 517 – 523.
16. A. M. Mamonov, S. V. Skvortsova, E. O. Agarkova, and O. Z. Umarova, "Physicochemical and technological bases of forming thermally stable structures of bimodal type in heat-resistant titanium alloys and alloys based on titanium aluminide with reverse alloying by hydrogen," *Titan*, No. 3, 9 – 15 (2013).
17. A. A. Il'in, S. Ya. Betsofen, S. V. Skvortsova, et al., "Structural aspects of ion nitriding of titanium alloys," *Metally*, No. 3, 6 – 15 (2002).
18. A. A. Il'in, S. V. Skvorstova, E. A. Lukina, et al., "Low-temperature ion nitriding of implants of titanium alloy VT20 in different structural states," *Metally*, No. 2, 38 – 44 (2005).
19. A. M. Mamonov, V. S. Spektor, E. A. Lukina, and S. M. Sarychev, "Use of vacuum ion plasma nitriding for improving medical implant wear resistance," *Titan*, No. 2, 45 – 50 (2010).
20. A. A. Il'in, V. K. Nosov, A. M. Mamonov, and V. N. Uvarov, "RF Patent 2081929, C1 MPK6 C 22 C 14/00, Alloy based on titanium aluminide, Claimant and patent holder Moscow Aviation Technological University im K. É. Tsiolkovsky, No. 95114327/02," *Byull. Izobr. Polezn. Modeli*, No. 17 (1997), claim 08.10.95, publ. 06.20.97.
21. *GOST 9.912–89. ESZKS. Corrosion-Resistant Steels and Alloys. Accelerated Test Method for Pitting Corrosion Resistance* [in Russian].
22. *ASTM G5–94. Standard Reference Test Method for Making Potentiostatic and Potentiodynamic Anodic Polarization Measurements* [in Russian].
23. A. A. Il'in, S. V. Svkortsova, V. S. Spektor, et al., "Low-temperature vacuum ion plasma nitriding of titanium alloys of different classes," *Tekhnol. Legk. Splavov*, No. 3, 103 – 110 (2008).
24. S. P. Belov, A. A. Il'in, A. M. Mamonov, and A. V. Aleksandrova, "Theoretical analysis of ordering processes in alloys based on Ti_3Al. 1. Mechanism of ordering in alloys based on compound Ti_3Al," *Metally*, No. 1, 134 – 138 (1994).
25. E. Etchessahar, I. P. Bars, and J. Debuigne, "Titanium nitrogen phase diagram and diffusion phenomenal," in: *Proc. 5th Int. Conf. on Titanium, Titanium Science and Technology*, Munich (1984), Vol. 3, pp. 1423 – 1440.